THM applied to the investigation of explosive astrophysical scenarios

IOP Conf. Series: Journal of Physics: Conf. Series **1308** (2019) 012012 doi:10.1088/1742-6596/1308/1/012012

THM applied to the investigation of explosive astrophysical scenarios.

M. La Cognata[1], S. Cherubini[1,2], M. Gulino[1,3], L. Lamia[1,2], R.G. Pizzone[1], S. Romano[1,2], C. Spitaleri[1], A. Tumino[1,3]

[1]Istituto Nazionale di Fisica Nucleare, Laboratori Nazionali del Sud, Via S. Sofia 62, Catania, 95123 Italy
[2]Dipartimento di Fisica e Astronomia "Ettore Majorana", Universitá di Catania, Via S. Sofia 64, Catania, 95123 Italy
[3]Facoltá di Ingegneria e Architettura, Universitá degli Studi di Enna "Kore", Cittadella Universitaria, Enna, 94100 Italy

E-mail: lacognata@lns.infn.it

Abstract. The Trojan Horse Method (THM) makes use of quasi-free reactions to deduce the cross section of nuclear reactions relevant for astrophysics at the energies of interest. Thanks to the suppression of the Coulomb barrier, the THM cross section does not exponentially vanishes at astrophysical energies. Here we will briefly summarise the fundamentals of the method, then we will discuss two applications of the method to reactions that have a pivotal role in the latest stages of stellar evolution, leading to explosive scenarios. In particular, we will focus on the indirect investigation of the ^{18}F$(p,\alpha)^{15}$O reaction, which is the most important ^{18}F destruction channel in novae, and the ^{12}C + ^{12}C reaction, which plays a critical role in astrophysics to understand stellar burning scenarios in carbon-rich environments, including supernovae.

1. The need of indirect techniques in nuclear astrophysics

Nuclear reaction cross sections $\sigma(E)$ have a pivotal role in modelling astrophysical phenomena since nuclear processes are responsible of energy production and synthesis of chemical elements in a variety of sites, ranging from the early universe to star's latest evolutionary stages. However, even at the highest astrophysical temperatures, reaching about 10^9 K, energies of interest are well below the Coulomb barriers of the fusing nuclei, in the case of reactions involving charged particles. Therefore, the Coulomb barrier strongly suppresses fusion cross sections, leading to vanishingly small signal-to-noise ratios. The building of underground laboratories has allowed, in few cases (see, for instance [1] for a review), to measure cross sections of astrophysical importance inside the energy window of astrophysical interest (the so-called Gamow window [2]). However, it turned out that at astrophysical energies, the presence of electrons cannot be neglected as the typical distances of closest approach are comparable to the atomic radii. The electron clouds surroundings projectile and target particles, usually in the form of partially stripped ions and atoms or molecules, respectively, screen the nuclear charges, determining an increase of the cross sections measured in the laboratory with respect to the case of bare nuclei. Such increase is described by an enhancement factor $f(E) = \exp\left(\pi\eta\frac{U_e}{E}\right)$, where U_e is the electron screening potential [3], which in the adiabatic limit (setting the upper limit for U_e), is calculated from the difference of the atomic binding energies in the fused system and in the separated atoms

[4]. However, many works (see, for instance, [5, 6, 7]) show that experimentally determined U_e values often exceed the theoretical upper limit, making it clear that our present understanding of the electron screening effect is far from being exhaustive.

Owing to the rapid change of cross sections with decreasing energies for charged-particle induced reactions, reaching values as small as picobarns, and to the uncertainties in magnitude due to the electron shielding, extrapolation, sometimes supported by theoretical calculations, is often the only possibility to have experimental estimates of nuclear cross sections at astrophysical energies. To this purpose, the astrophysical factor is usually adopted [3], $S(E) = \sigma(E)\, E\, \exp(2\pi\eta)$, where $\eta = \mathrm{Z_1 Z_2} e^2/\hbar v$ is the Sommerfeld parameter, $\mathrm{Z_1}$ and $\mathrm{Z_2}$ the atomic numbers of the interacting nuclei and v their relative velocity. Thanks to the introduction of the exponential factor, the main energy dependence of the cross section is compensated for and, as a consequence, $S(E)$ is a smooth function of the energy in the case of non resonant reactions.

However, resonant reactions play an important role in astrophysics as they might significantly increase the astrophysical factor, even by orders of magnitude, and alter nucleosynthesis and energy production, if resonances occur at energies of astrophysical interest. Therefore, unexpected resonances or inaccurate estimates of their strengths might introduce large systematic errors, making extrapolation very risky. A special role is played by broad sub threshold resonances. Even if resonance energies are lower than the entrance channel separation energy, resonance tails can be populated, causing an exponential increase of the astrophysical factor for center-of-mass energies approaching zero. Also in this case extrapolation is very challenging, owing to the unknown resonance strengths as well as to the interplay with the electron screening effect, also determining a steep rise of the astrophysical factor at energies close to the threshold. An important example is given by the measurement of the $^{13}\mathrm{C}(\alpha, n)^{16}\mathrm{O}$ S-factor (see, for instance, [8, 9, 10]), which is dominated by the tail of the $1/2^+$ $^{17}\mathrm{O}$ state at 6.356 MeV at astrophysical energies ($140 - 230$ keV).

It is also worth noting that the investigation of near threshold regions has important implications for nuclear structure. Indeed, resonances are caused by states in the intermediate compound nucleus formed in the reaction and their study makes it possible to deduce resonance energies, spin-parities and partial widths. Besides being difficult to investigate, the near threshold region is important as cluster structures are especially likely to appear right at these energies. Therefore, the introduction of alternative approaches such as indirect methods, in the exploration of nuclear reactions at astrophysical energies, has led to invaluable contribution in the understanding of nuclear astrophysics and nuclear structure. In what follows, we will focus on the Trojan horse method, established as a tool to investigate low-energy nuclear reactions by C. Spitaleri [11].

In recent years, the THM has been applied to reactions involved in quiescent nuclear burning, often involving low-energy proton-induced reactions (see, for instance, the recent review [12]). However, also in the case of explosive scenarios, when typical temperatures can be as large as 10^9 K and radioactive nuclei play an important role, THM represents a valuable technique to access the energies of astrophysical interest. Even if cross sections are generally larger than those characterising hydrostatic burning, yet the presence of high Z nuclei and/or radioactive species still makes direct measurement very challenging because of the small cross sections and of the low beam intensities, respectively.

2. Basic features of the resonant THM

The aim of the THM is to deduce the astrophysical factor of the $A(x, b)B$ reaction by studying a $A(a, bB)s$ process performed at energies of a few AMeV, namely, larger than the $A - a$ Coulomb barrier. Therefore, it is possible to bypass Coulomb and centrifugal barriers and electron screening effects (see [5] and references therein about the electron screening problem).

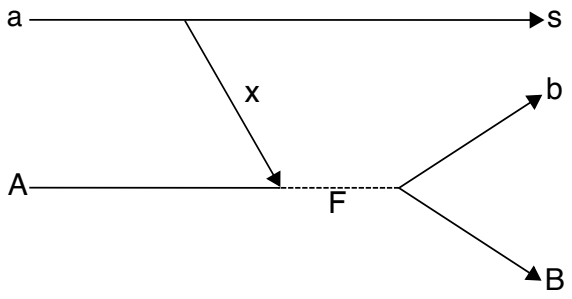

Figure 1. Sketch of the QF $A(a,bB)s$ reaction, used to transfer a cluster x off the particle a and populate excited states of nucleus F, later decaying to $b+B$.

Yet, astrophysical energies in the $A-x$ channel can be reached thanks to the energy paid to break the nucleus $a=x+s$. Such system, usually referred to as the Trojan Horse (TH) nucleus, has to show a large $x-s$ cluster structure. In a simplified picture, since the Coulomb and centrifugal barriers are overcome in the $A-a$ channel, the $A(x,b)B$ reaction takes place in the nuclear field so it is not hindered by Coulomb and centrifugal repulsion. In order to achieve a simple connection between the $A(a,bB)s$ cross section and the one of astrophysical interest ($A(x,b)B$), the quasi-free (QF) contribution to the $2\rightarrow 3$ cross section has to be singled out, namely, a participant-spectator mechanism. This leads to the population of excited states of the intermediate nucleus $F=A+x$, later decaying into $b+B$, where x is coming from the virtual breakup of the TH nucleus a. An additional advantage is that the $x-s$ intercluster motion can be used to further reduce the $A-x$ relative energy (even reaching negative values by a careful choice of the kinematic variables[9]), as well as to span a broad $A-x$ relative energy interval even if a single beam energy is used, which is particularly useful in the case of radioactive ion beams [13, 14, 15] and neutrons [16].

In a graphical representation, the reaction mechanism sketched in Fig.1 has to be selected, namely, the participant (x)-spectator (s) process where the TH nucleus undergoes direct breakup and s is emitted without influencing the $A(x,b)B$ sub-reaction.

In the original theoretical formulations of the THM (see, for instance [17]), it was pointed out that for each contributing partial wave to the $A(x,b)B$ virtual reaction, the corresponding penetration factor $P_l(k_{xA},R_{xA})$ (k_{xA} and R_{xA} being the $A-x$ channel wave number and radius, respectively) and normalization constant $N_{l,\,Ax}$ have to be multiplied to the $A(x,b)B$ cross section, obtained using the THM, to compare it with the directly measured one:

$$\frac{d\sigma}{d\Omega}=\sum_l N_{l,\,Ax}P_l(k_{xA},R_{xA})\frac{d\sigma^{HOES}_{Ax\rightarrow bB}}{d\Omega}\,. \tag{1}$$

In this formula, $d\sigma^{HOES}_{Ax\rightarrow bB}/d\Omega$ is the half-off-energy-shell (HOES) THM cross section, which is deduced from the THM data, since the participant x is a virtual particle that does not satisfy the mass-shell equation [22].

Of course, in the case of multi resonant reactions, such an approach may introduce large normalization errors, since it is necessary to determine a scaling constant for each contributing wave [17]. When many resonances are present, populated in a variety of orbital angular momenta, an extension of the THM to account for multiple wave contribution and normalization to the direct data is mandatory. After the seminal work [18], extensive theoretical [19, 20] and experimental [21, 22] studies were performed to develop and validate a novel approach to treat multi-resonance reactions, named modified R-matrix approach. This is a generalisation of the R-matrix [23] because we consider reactions with three particles in the exit channel, where the

TH-nucleus a in the initial state carries the transferred particle x, which is off-the-energy-shell.

In the plane wave approximation, the amplitude of the process $a + A \to b + B + s$ (Fig.1) is:

$$M^{PWA(prior)}(P, \mathbf{k}_{aA}) = \left\langle \chi^{(0)}_{sF} \Psi^{(-)}_{bB} | V_{xA} | \varphi_a \varphi_A \chi^{(0)}_{aA} \right\rangle , \tag{2}$$

where $P = (\mathbf{k}_{sF}, \mathbf{k}_{bB})$ is the six-dimensional momentum describing the three-body system s, b and B. $\chi^{(0)}_{aA} = \exp(i\mathbf{k}_{aA} \cdot \mathbf{r}_{aA})$, $\chi^{(0)}_{sF} = \exp(i\mathbf{k}_{sF} \cdot \mathbf{r}_{sF})$, $\mathbf{r}_{ij}$ and $\mathbf{k}_{ij}$ are the relative coordinate and relative momentum of i and j nuclei, $\Psi^{(-)}_{bB}$ is the wave function of the nuclei b and B in the exit channel, $F = b + B$, V_{xA} is the interaction potential of x and the target nucleus A, φ_a and φ_A are the a and A bound state wave functions, respectively. Assuming that the reaction yield is dominated by resonances, the plane wave amplitude from which the THM cross section is calculated is given by Refs. [24, 20]:

$$\begin{aligned}
M^{PWA(prior)}(P, \mathbf{k}_{aA}) = (2\pi)^2 \sqrt{\frac{1}{\mu_{bB} k_{bB}}} \varphi_a(\mathbf{p}_{sx}) \\
\times \sum_{J_F M_F j' l l' m_{j'} m_l m_{l'} M_x} i^{l+l'} \langle j m_j l m_l | J_F M_F \rangle \langle j' m_{j'} l' m_{l'} | J_F M_F \rangle \\
\times \langle J_x M_x J_A M_A | j' m_{j'} \rangle \langle J_s M_s J_x M_x | J_a M_a \rangle \\
\times \exp\left[-i\delta^{hs}_{bB\,l}\right] Y_{l m_l}(-\hat{\mathbf{k}}_{bB}) \\
\times \sum_{\nu\tau=1}^{N} \left[\Gamma_{\nu bBjlJ_F}\right]^{1/2} \left[\mathbf{A}^{-1}\right]_{\nu\tau} Y^*_{l'm'}(\hat{\mathbf{p}}_{xA}) \\
\times \sqrt{\frac{R_{xA}}{\mu_{xA}}} \left[\Gamma_{\nu xAl'j'J_F}(E_{xA})\right]^{1/2} P^{-1/2}_{l'}(k_{xA}, R_{xA}) \\
\times \left(j_{l'}(p_{xA}R_{xA}) \left[(B_{xA\,l'}(k_{xA}, R_{xA}) - 1) - D_{xA\,l'}(p_{xA}, R_{xA})\right] \right. \\
\left. + 2Z_x Z_A e^2 \mu_{xA} \int_{R_{xA}}^{\infty} \mathrm{d}r_{xA} \frac{O_{l'}(k_{xA}, r_{xA})}{O_{l'}(k_{xA}, R_{xA})} j_{l'}(p_{xA} r_{xA}) \right) .
\end{aligned} \tag{3}$$

Here, $F = b + B$, μ_{ij} is the $i - j$ reduced mass, r_{ij} is the $i - j$ relative distance, $\mathbf{p}_{ij}$ is the $i - j$ relative momentum in the case of off-energy-shell particles, thus $E_{ij} \neq p^2_{ij}/2\mu_{ij}$ (while $\mathbf{k}_{ij}$ is calculated assuming the particles on-shell), $\delta^{hs}_{bB\,l}$ is the solid sphere scattering phase shift, R_{xA} the $x + A$ channel radius,

$$B_{xA\,l'}(k_{xA}, R_{xA}) = R_{xA} \frac{\frac{\partial O_{l'}(k_{xA}, R_{xA})}{\partial r_{xA}}|_{r_{xA}=R_{xA}}}{O_{l'}(k_{xA}, R_{xA})} \tag{4}$$

is the logarithmic derivative as in the R-matrix method,

$$O_{l'}(k_{xA}, R_{xA}) = \sqrt{\frac{k_{xA} R_{xA}}{P_{l'}(k_{xA}, R_{xA})}} \exp\left[-i\delta^{hs}_{xA\,l'}\right] \tag{5}$$

is the outgoing spherical wave,

$$D_{xA\,l'}(p_{xA}, R_{xA}) = R_{xA} \frac{\frac{\partial j_{l'}(p_{xA}, R_{xA})}{\partial r_{xA}}|_{r_{xA}=R_{xA}}}{j_{l'}(p_{xA}, R_{xA})} \tag{6}$$

is the logarithmic derivative and $j_{l'}(p_{xA}, R_{xA})$ the spherical Bessel function, N the number of the included levels.

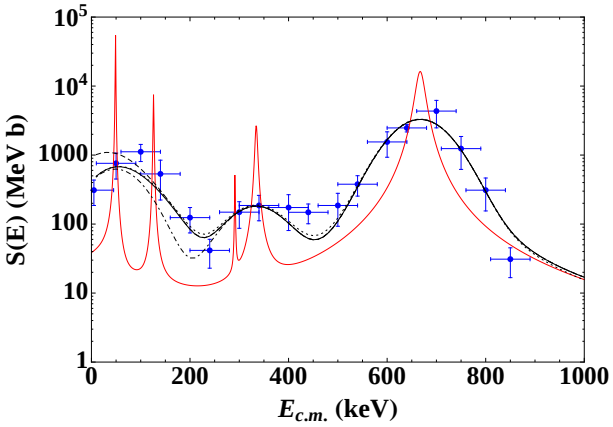

Figure 2. R-matrix analysis of the THM astrophysical factor (blu points), under the assumption of $J^{\pi} = 3/2^{+}$ for the 6460 keV ^{19}Ne state [14]. The solid black line is the smoothed R-matrix calculation, accounting for a 53 keV energy spread (standard deviation). The red line is the corresponding deconvoluted astrophysical factor. The dashed black line is the smoothed R-matrix calculation including the 6417 keV level, while the dot-dashed line is the smoothed R-matrix calculation where the 6537 keV is excluded. Finally, the dotted line marks the smoothed R-matrix calculation where the interference signs were changed to (++)(-+). The figure is taken from [15].

Eq.3 contains the same level matrix $\mathbf{A}_{\nu\tau}$ as in the standard R-matrix theory [23], thus the same energies and reduced width amplitudes. Therefore, from the HOES cross section it is possible to deduce the on-energy-shell (OES) one with no need of extrapolation, accounting for the virtual nature of the transferred particle and energy resolution effects. Also, in the plane wave approximation the OES cross section is obtained in arbitrary units; however, normalization to direct data is gained by scaling the reduced γ-widths of indirectly measured resonances to the ones of states lying at high energy and accurately known from the literature, independently from the corresponding orbital angular momenta (see [25]). Another important feature is the possibility to measure down to zero energy, even in the case of charged-particle induced reactions, which is accomplished thanks to the appearance of the $P_{l'}^{-1/2}(k_{xA}, R_{xA})$ factor in Eq.3, namely the inverse penetration factor.

3. The ^{18}F$(p,\alpha)^{15}$O reaction studied with the THM

Crucial information on nova nucleosynthesis can be potentially inferred from γ-ray signals powered by ^{18}F decay [26]. The ^{18}F$(p,\alpha)^{15}$O cross section has been measured by means of several dedicated experiments, being a major ^{18}F destruction channel. However, the present uncertainty on the cross section at astrophysical energies, below about $\sim$ 300 keV is far from satisfactory, owing to the need of radioactive ^{18}F beam. Thanks to the suppression of the Coulomb barrier, the THM proved very well suited to span the whole energy interval in a single measurement [13, 14]. Then, following [27], we performed a R-matrix analysis of the THM data to check the compatibility of the THM S-factor with this recent R-matrix calculation, accounting for most of recent direct and indirect results and spectroscopic information.

The THM S(E) factor is shown as blue circles in Fig.2. The best fit of the THM data [13, 14] was achieved by assuming the (++)(++) interference pattern (using the same notation as in [27]), by excluding the 7 keV resonance, due to the $3/2^{-}$ state of ^{19}Ne at 6417 keV energy, and by introducing the $7/2^{+}$ state of ^{19}Ne at 6537 keV, whose occurrence was pointed out in [13, 14]. In detail, the (++)(++) notation is used when the relative interference signs between the -124 keV

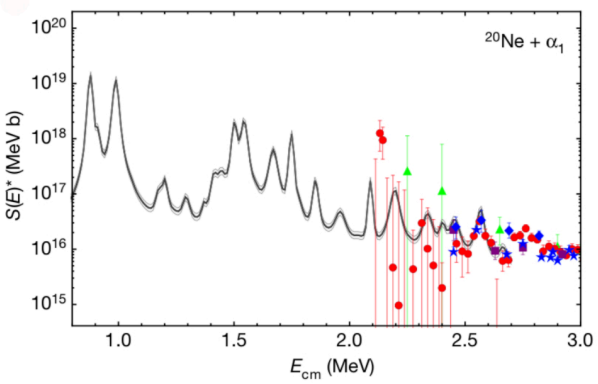

Figure 3. THM ^{12}C(^{12}C, α_1)^{20}Ne modified astrophysical factor S^* (gray band), compared with the available direct data (solid symbols). See Ref.[33] for a detailed discussion.

and 1461 keV resonances in the ^{18}F$(p,\alpha)^{15}$O cross section is (++) (first pair) and the ones of the 47 and 665 keV resonances is (++) as well (second pair). The list of levels used in the calculations is given in Tab.1 of [15], while the resulting best fit astrophysical factor is marked by a red line in Fig.2 in the case of infinite energy resolution, and by a black solid line including the effect of experimental energy resolution (53 keV standard deviation, [13]). For 18 degrees of freedom, a reduced $\chi^2 = 1.5$ is obtained. The present result is not much sensitive on the change of the interference pattern from the (++)(++) relative signs to the (++)(-+) combination, that is, assuming constructive interference between the $3/2^+$ states (dotted line in Fig.2), thanks to the occurrence of the 126 keV peak. Instead, the inclusion of the 6417 keV state (dashed black line) or the removal of the 6537 keV one (dot-dashed black line) cause a significant increase of the reduced χ^2, suggesting that such alternative solutions should be discarded.

4. The ^{12}C + ^{12}C reactions

^{12}C + ^{12}C fusion is a key process in nuclear physics and astrophysics. Indeed, it has been extensively investigated (see Ref. [28] and references therein) to understand fusion reaction mechanism, especially to pinpoint the occurrence and origin of the fusion hindrance (see, for instance, Ref.[29]). In astrophysics, the ^{12}C + ^{12}C fusion rate bears a great importance in the evolution of massive stars ($M_\odot \geq 8$), especially in the case of objects in late evolutionary stages. At present, direct data are present down to about 2.5 MeV center-of-mass energies (at lower energies uncertainties are so large that they are not statistically significant [28]), so extrapolation is necessary to supply the astrophysical factor at the energies of interest, especially for astrophysics, comprised between about 1−2 MeV. Extrapolations are usually performed using the modified astrophysical S-factor [30]:

$$S^* = E\,\sigma(E)\exp(2\pi\eta + g\,E)\,, \tag{7}$$

where $\eta = 13.88\,E^{-1/2}$ and $g = 0.46$ MeV^{-1} (the center-of-mass energy E being expressed in MeV).

However, the large uncertainties affecting direct data close to astrophysical energies and the presence of oscillations in the modified astrophysical factor make extrapolation quite unreliable, especially because the reaction mechanism (for instance, the possibility that fusion hindrance suppresses the cross section to values lower than predicted by coupled-channel calculations [29]). In the case of ^{12}C+^{12}C, measurements below 2 MeV are hampered because the Coulomb barrier

reduces the cross section to values as low as few nanobarns already at $E = 2.5$ MeV, because of the strong background especially due to the deuterium content in the targets [28] and because of the effect of energy loss in the targets themselves, making it difficult to fix the correct interaction energy [31]. For all these reasons, we decided to carry out a THM measurement, which can bypass all the mentioned problems thanks to its indirect approach. Indeed, while the Coulomb suppression is overcome as discussed in Sect.2, the use of reactions with three particles in the exit channel makes it possible to reconstruct the reaction Q-value and select only the events from the reaction of interest, essentially background free. Also, the use of comparatively higher energies than the astrophysical ones make the ambiguity in interaction energy determination negligible.

Since the possibility of using ^{14}N to transfer a ^{12}C nucleus is well known (see, for instance, [32]), we investigated $^{12}C + {}^{12}C$ fusion by applying the THM to the $^{14}N + {}^{12}C$ reactions [33]. The experiment was carried out at the *Laboratori Nazionali del Sud, Istituto Nazionale di Fisica Nucleare* (Catania, Italy) using a 30 MeV ^{14}N beam delivered by the Van de Graff Tandem accelerator. We were able to measure the cross sections for the $^{12}C(^{12}C, \alpha_0)^{20}Ne$, $^{12}C(^{12}C, \alpha_1)^{20}Ne$, $^{12}C(^{12}C, p_0)^{23}Na$ and $^{12}C(^{12}C, p_1)^{23}Na$ channels in arbitrary units, covering the energy range of astrophysical interest and a region above about 2.5 MeV. This is necessary to normalize the THM data to the direct ones, so an energy interval where they are less affected by statistical and systematic errors is chosen, to obtain the THM S^* factors and minimize systematics errors. The THM measurement made it possible to perform a validity test of the method, thanks to the precise matching of the trend of the experimental direct and indirect data in the overlapping energy region, and to shed light on the trend of S^* below about 2 MeV, where a definite resonant pattern was observed, whose interesting physical consequences are being addressed by several authors [34, 35]. In particular, fig.3 from [33] shows the $^{12}C(^{12}C, \alpha_1)^{20}Ne$ S^*-factor obtained by applying Eq.3, superimposed to the available direct data (filled circles[36], filled squares[37], empty diamonds[38], filled stars[39] and filled triangles[40]). Other approaches, such as those sketched in Refs. [41, 42], presently fail to satisfy such necessary condition, as shown in Ref. [43], demonstrating once again the robustness of THM.

References

[1] Broggini C et al. 2018 *Progress in Particle and Nuclear Physics* **98** 55
[2] Iliadis C 2007 *Nuclear Physics of Stars* (New York: Wiley)
[3] Rolfs C E and Rodney W S 1998 *Cauldrons in the cosmos: Nuclear astrophysics* (Chicago: University of Chicago Press)
[4] Bracci L et al. 1990 *Nucl. Phys. A* **513** 316
[5] La Cognata M et al. 2005 *Phys. Rev. C* **72** 065802
[6] Rinollo A et al. 2005 *Nucl. Phys. A* **758** 146C
[7] Tumino A et al. 2011 *Phys. Lett. B* **705** 546
[8] La Cognata M et al. 2012 *Phys. Rev. Lett.* **109** 232701
[9] La Cognata M et al. 2013 *The Astrophysical Journal* **777** 143
[10] Trippella O and La Cognata M 2017 *The Astrophysical Journal* **837** 41
[11] Spitaleri C 1991 *Proceedings of the 5Th Winter School on Hadronic Physics: Problems of Fundamental Modern Physics II* (Singapore: World Scientific) 21
[12] Spitaleri C et al. 2016 *Eur. Phys. J. A* **52** 77
[13] Cherubini S et al. 2015 *Phys. Rev. C* **92** 015805
[14] Pizzone R G et al. 2016 *Eur. Phys. J. A* **52** 24
[15] La Cognata M 2017 *The Astrophysical Journal* **846** 65
[16] Gulino M et al. 2013 *Phys. Rev. C* **87** 012801
[17] Typel S et al. 2003 *Annals of Physics* **305** 228
[18] La Cognata M 2008 *Phys. Rev. Lett.* **101** 152501
[19] Mukhamedzhanov A M et al. 2008 *Journal of Physics G Nuclear Physics* **35** 014016
[20] Mukhamedzhanov A M 2011 *Phys. Rev. C* **84** 044616
[21] La Cognata M et al. 2010 *Astrophys. J.* **723** 1512
[22] La Cognata M et al. 2009 *Phys. Rev. C* **80** 012801

[23] Lane A M and Thomas R G 1958 *Rev. Mod. Phys.* **30** 257
[24] Tribble R E et al. 2014 *Reports on Progress in Physics* **77** 106901
[25] La Cognata M et al. 2015 *Astrophys. J.* **805** 128
[26] José, J 2016 *Stellar Explosions: Hydrodynamics and Nucleosynthesis* (Boca Raton, FL, London: CRC/Taylor and Francis)
[27] Bardayan D W et al. 2015*Phys. Lett. B* **751** 311
[28] Zickefoose J et al. 2018 *Phys. Rev.* C **97** 065806
[29] Jiang C L et al. 2002 *Phys. Rev. Lett.* **89** 052701
[30] Patterson J R et al. 1969 *The Astrophysical Journal* **157** 367
[31] Fisichella M et al. 2015 *Phys. Rev.* C **92** 064611
[32] Artemov K P et al. 1984 *Phys. Lett. B* **149** 325
[33] Tumino A et al. 2018 *Nature* **557** 687
[34] Mori K et al. 2019 *Monthly Notices of the Royal Astronomical Society: Letters* **482** L70
[35] Straniero O et al. 2019 arXiv:1901.00173
[36] Spillane T et al. 2007 *Phys.Rev. Lett.* **98** 122501
[37] Mazarakis M G et al. 1973 *Phys. Rev.* C **7** 1280
[38] High M D et al. 1977 *Nucl. Phys.* A **282** 181
[39] Kettner K U et al. 1980 *Z. Phys.* A **298** 65
[40] Barron-Palos L et al. 2006 *Nucl. Phys.* A **779** 318
[41] Mukhamedzhanov A M and Pang D Y 2018 arXiv:1806.08828v4
[42] Mukhamedzhanov A M et al. 2018 arXiv:1806.05921v1
[43] Tumino A et al. 2018 arXiv:1807.06148v1